Journal of Low Temperature Physics (2019) 196:126–132
https://doi.org/10.1007/s10909-018-02114-1

Single-Particle Structures in the Normal State of a Strongly Interacting Bose–Fermi Mixture with Mass Imbalance

K. Manabe[1] · D. Kagamihara[1] · D. Inotani[1] · Y. Ohashi[1]

Received: 28 June 2018 / Accepted: 2 December 2018 / Published online: 13 December 2018

Abstract
We extend some of the authors' previous work for a mass-balanced Bose–Fermi mixture to include effects of realistic mass imbalance in a ^{23}Na–^{40}K and a ^{87}Rb–^{40}K mixtures. Including effects of pairing fluctuations within the framework of an improved T-matrix theory, we calculate the single-particle spectral weight (SW), as well as the photoemission spectrum (PES) in the unitary regime at the Bose–Einstein condensation temperature $T_{\rm BEC}$. We show that the characteristic three-peak structure induced by paring fluctuations, being predicted in the mass-balanced case, remains to exist in SW even in the presence of mass difference. We also show that PES is a useful experimental method to observe this phenomenon in a ^{23}Na–^{40}K, as well as ^{87}Rb–^{40}K, Bose–Fermi mixtures. Since this strong-coupling phenomenon is qualitatively different from that in a two-component Fermi gas, our results would be useful in clarifying how the quantum statistics affects Bose and Fermi pairing phenomena in a two-component gas mixture.

Keywords Cold atom physics · Bose–Fermi mixture · Bose–Einstein condensation · Strong-coupling effects

1 Introduction

A Bose–Fermi gas mixture consisting of single-component Bose and Fermi atoms [1–5] has recently attracted much attention as a counterpart of a two-component Fermi gas. In both the cases, one can tune the strength of a pairing interaction between different components by using a Feshbach resonance [6]. This novel technique enables us to systematically investigate an analogous paring phenomenon in a Bose–Fermi mixture to the so-called BCS-BEC crossover [7,8] discussed in the Fermi–Fermi case.

✉ K. Manabe
k.manabe.rikou@keio.jp

[1] Department of Physics, Faculty of Science and Technology, Keio University, 3-14-1 Hiyoshi, Kohoku-ku, Yokohama 223-8522, Japan

A crucial difference between the Bose–Fermi and Fermi–Fermi cases are quantum-statistical properties of atomic species in these systems. For example, in the Fermi–Fermi case, Fermi atoms form molecular bosons, to be experienced the superfluid transition, that occurs at a higher temperature in the strong-coupling regime than in the weak-coupling regime. On the other hand, in a Bose–Fermi mixture, Fermi molecules are formed by a Bose–Fermi pairing interaction that suppresses the Bose–Einstein condensation of Bose atoms, because of the decrease in the number of unpaired bosons. Thus, it is an interesting issue how such quantum-statistical difference affects physical properties of a two-component gas mixture. In this regard, some of the authors have recently shown that, in the simplest mass-balanced case, the detailed spectral structure of single-particle spectrum weight (SW) near the Bose–Einstein condensation temperature $T_{\rm BEC}$ in a Bose–Fermi mixture is very different from the case of a two-component Fermi gas. That is, while SW in the latter case exhibits a double peak structure along the particle dispersion and the hole dispersion that are coupled by paring fluctuations, SW in the former case has three-peak lines along the particle dispersion, hole dispersion, and dispersion of a composite Fermi molecule [9,10]. As mentioned in Ref. [11], this third peak comes from the fact that bosons start to gather into the zero-momentum state near $T_{\rm BEC}$.

In this paper, we extend the above-mentioned previous work for a mass-balanced Bose–Fermi mixture to the case with a mass imbalance. This extension is really important, because a real Bose–Fermi mixture is always accompanied by mass imbalance. In particular, this paper deals with the case of ^{23}Na–^{40}K and ^{87}Rb–^{40}K mixtures, that have already been realized[2–5] . In addition, from the viewpoint of observation, SW discussed in Ref. [11] is *not* observable in the current experimental technology in cold atom physics. The nearest observable quantity in this field is the photoemission spectrum (PES) [12–14]. Including this experimental situation, we thus examine PES, in addition to SW. For strong Bose–Fermi hetero-pairing fluctuations, we take into these within the framework of the improved T-matrix approximation(iTMA) developed in Refs. [11,15]. Throughout this paper, we set $\hbar = k_{\rm B} = 1$, and the system volume V is taken to be unity, for simplicity.

2 Formalism

We consider a Bose–Fermi mixture consisting of single-component Bose and Fermi atoms with a contact-type attractive interaction, described by the Hamiltonian,

$$H = \sum_{\boldsymbol{p},s={\rm B,F}} \xi^s_{\boldsymbol{p}} c^\dagger_{\boldsymbol{p},s} c_{\boldsymbol{p},s} - U_{\rm BF} \sum_{\boldsymbol{p},\boldsymbol{p}',\boldsymbol{q}} c^\dagger_{\boldsymbol{p}+\boldsymbol{q},{\rm B}} c^\dagger_{\boldsymbol{p}'-\boldsymbol{q},{\rm F}} c_{\boldsymbol{p}',{\rm F}} c_{\boldsymbol{p}{\rm B}}. \tag{1}$$

$c^\dagger_{\boldsymbol{p},s={\rm B,F}}$ is a creation operator of a Bose ($s = {\rm B}$) and a Fermi ($s = {\rm F}$) atom with the momentum $\boldsymbol{p}$, and the kinetic energy $\xi^s_{\boldsymbol{p}} = p^2/(2m_s) - \mu_s$, measured from the chemical potential μ_s(note that the "pseudospin" s =B,F describes boson and fermion in the present case). As mentioned previously, we consider the case when a fermion mass $m_{\rm F}$ is different from a boson mass $m_{\rm B}$ ($m_{\rm B}/m_{\rm F} \neq 1$). In particular, we set

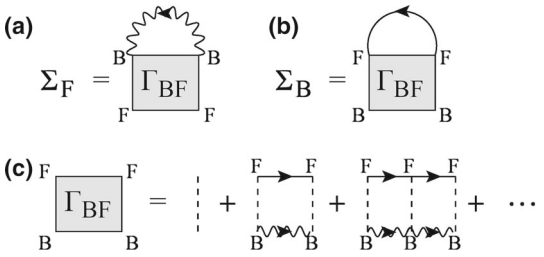

Fig. 1 Fermi (**a**) and Bose (**b**) self-energy corrections in iTMA. The solid line represents the bare Fermi Green's function $G_F^0 = [i\omega_F - \xi_{\boldsymbol{p}}^F]^{-1}$. The wavy line is the *modified* Bose Green's function $\tilde{G}_B^0$ in Eq. (4). The dashed lines denote a bare hetero-pairing interaction $-U_{BF}$. **c** iTMA particle–particle scattering matrix Γ_{BF}

$m_B/m_F = 23/40(< 1)$ in a ^{23}Na–^{40}K mixture, as well as $m_B/m_F = 87/40(> 1)$ in a ^{87}Rb–^{40}K mixture. $-U_{BF}(< 0)$ is a tunable pairing interaction between Bose and Fermi atoms associated with a Feshbach resonance. In this paper, we ignore a weak repulsive interaction between Bose atoms, for simplicity. Regarding this, we note that, in the normal state (which we are considering in this paper), the main effect of this interaction is merely a mean-field shift of the Bose chemical potential, so that the inclusion of this effect would not drastically change spectral properties of the system[16–18]. When we extend the present work to the superfluid phase, however, one should include such a Bose–Bose interaction, because it is crucial for the stability of Bose superfluids. We also note that a contact-type s-wave interaction does not exist between Fermi atoms due to the Pauli exclusion principle. As usual, the interaction strength is measured in terms of the s-wave scattering length a_{BF}, which is related to the bare interaction $-U_{BF}$ as,

$$a_{BF} = \frac{-U_{BF}}{1 - U_{BF}\sum_{\boldsymbol{p}}^{p_c} \frac{2m_r}{p^2}}, \tag{2}$$

where $m_r = (1/m_B + 1/m_F)^{-1}$ is the reduced mass.

In considering single-particle properties of this hetero atomic gas, it is convenient to consider the single-particle thermal Green's function given by

$$G_s(\boldsymbol{p}, i\omega_s) = \frac{1}{i\omega_s - \xi_{\boldsymbol{p}}^s - \Sigma_s(\boldsymbol{p}, i\omega_s)}. \tag{3}$$

Here, $\omega_B(\omega_F)$ is the Bose (Fermi) Matsubara frequency. The self-energy correction $\Sigma_{s=B,F}(\boldsymbol{p}, i\omega_s)$ involves effects of Bose–Fermi pairing fluctuations associated with the pairing interaction $-U_{BF}$. In iTMA [11,15], Σ_F and Σ_B are diagrammatically given in Fig. 1a, b, respectively. In these diagrams, the particle–particle scattering matrix Γ_{BF} given in panel (c) physically describes hetero-pairing fluctuations, where the formation and dissociation of composite Fermi molecules repeatedly occur. Although the diagrammatic structure in Fig. 1 is formally the same as that in the ordinary T-matrix approximation (TMA) [16–19], we note that iTMA uses the *modified* Bose Green's function,

$$\tilde{G}_{\rm B}^{0}(\boldsymbol{p}, i\omega_{\rm B}) = \frac{1}{i\omega_{\rm B} - \xi_{\boldsymbol{p}}^{\rm B} - \Sigma_{\rm B}(\boldsymbol{0}, 0)}, \tag{4}$$

in the diagrams in Fig. 1. Then the required gapless conditions are always guaranteed at $T_{\rm BEC}$ when the Hugenholtz–Pines condition,

$$\mu_{\rm B} - \Sigma_{\rm B}(\boldsymbol{0}.0) = 0 \tag{5}$$

is satisfied [20]. Regarding this, the ordinary TMA uses the bare Bose Green's function $G_{\rm B}^{0}(\boldsymbol{p}, i\omega_{\rm B}) = \left[i\omega_{\rm B} - \xi_{\boldsymbol{p}}^{\rm B}\right]^{-1}$ in Fig. 1, so that the Bose excitations are still gapped even at $T_{\rm BEC}$.

Summing up the diagrams in Fig. 1, we obtain,

$$\Sigma_{\rm F}(\boldsymbol{p}, i\omega_{\rm F}) = -T\sum_{\boldsymbol{q}, \omega_{\rm F}'} \Gamma_{\rm BF}(\boldsymbol{q}, i\omega_{\rm F}')\tilde{G}_{\rm B}^{0}(\boldsymbol{q} - \boldsymbol{p}, i\omega_{\rm F}' - i\omega_{\rm F}), \tag{6}$$

$$\Sigma_{\rm B}(\boldsymbol{p}, i\omega_{\rm B}) = T\sum_{\boldsymbol{q}, \omega_{\rm F}'} \Gamma_{\rm BF}(\boldsymbol{q}, i\omega_{\rm F}')G_{\rm F}^{0}(\boldsymbol{q} - \boldsymbol{p}, i\omega_{\rm F}' - i\omega_{\rm B}). \tag{7}$$

Here, the Bose–Fermi scattering matrix $\Gamma_{\rm BF}(\boldsymbol{q}, i\omega_{\rm F}')$ has the form,

$$\Gamma_{\rm BF}(\boldsymbol{q}, i\omega_{\rm F}') = \frac{-U_{\rm BF}}{1 - U_{\rm BF}\Pi_{\rm BF}(\boldsymbol{q}, i\omega_{\rm F}')}, \tag{8}$$

where

$$\Pi_{\rm BF}(\boldsymbol{q}, i\omega_{\rm F}') = T\sum_{\boldsymbol{k}, i\omega_n} G_{\rm F}^{0}(\boldsymbol{q} - \boldsymbol{k}, i\omega_{\rm F}' - i\omega_n)\tilde{G}_{\rm B}^{0}(\boldsymbol{k}, i\omega_n) \tag{9}$$

is the lowest order hetero-pair correlation function.

As usual, the Bose–Einstein condensation temperature $T_{\rm BEC}$ is conveniently determined from the Hugenholtz–Pines theorem in Eq.(5), stating the gapless Bose excitations in the BEC phase. We actually solve Eq.(5), together with the equation for the number $N_{\rm F}$ of Fermi atoms,

$$N_{\rm F} = T\sum_{\boldsymbol{p}, i\omega_{\rm F}} G_{\rm F}(\boldsymbol{p}, i\omega_{\rm F})e^{i\omega_{\rm F}\delta}, \tag{10}$$

as well as the number $N_{\rm B}$ of Bose atoms,

$$N_{\rm B} = -T\sum_{\boldsymbol{p}, i\omega_{\rm B}} G_{\rm B}(\boldsymbol{p}, i\omega_{\rm B})e^{i\omega_{\rm B}\delta}, \tag{11}$$

to self-consistently determine $T_{\rm BEC}$, $\mu_{\rm F}$, and $\mu_{\rm B}$. For simplicity, we take $N_{\rm F} = N_{\rm B} = N$ in this paper (population-balanced case). Once these quantities are determined, the single-particle spectral weight $A_{\rm F}(\boldsymbol{p}, \omega)$, as well as the photoemission spectrum

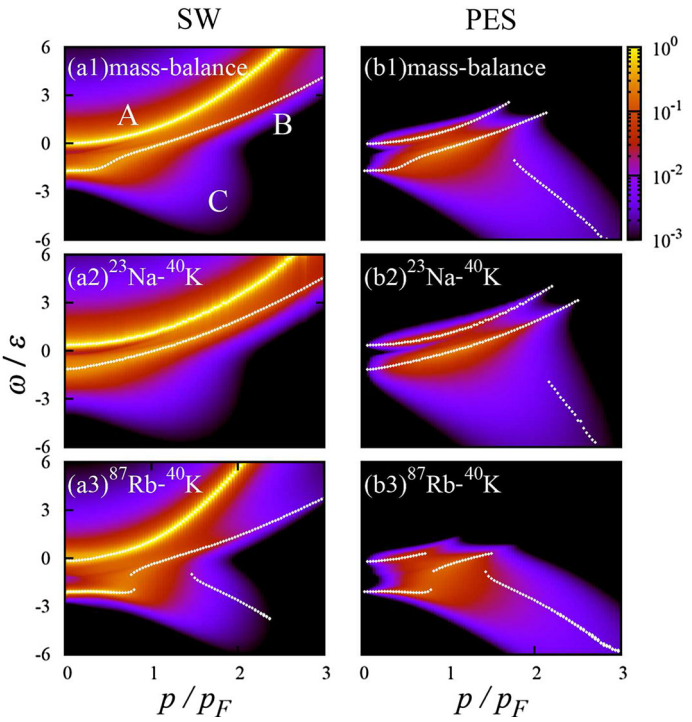

Fig. 2 Calculated intensity of the Fermi spectral weight (SW) $A_{\rm F}(\boldsymbol{p}, \omega)$ (left panels) and the photoemission spectrum (PES) $p^2 A_{\rm F}(\boldsymbol{p}, \omega) f(\omega)$ (right) in a Bose–Fermi mixture. We set $(k_{\rm F} a_s)^{-1} = 0.1$ (unitary regime) and $T = T_{\rm BEC}$. SW is normalized by ϵ, twice the Fermi energy of composite Fermi molecule. **a1**, **b1** a mass-balanced case ($m_{\rm B} = m_{\rm F}$). **a2**, **b2** ^{23}Na–^{40}K mixture. **a3**, **b3** ^{87}Rb–^{40}K mixture. The white dotted lines show the peak positions of the spectrum (Color figure online)

(PES) $I_{\rm F}(\boldsymbol{p}, \omega)$, in the Fermi channel are calculated from the analytic-continued iTMA Green's function $G_{\rm F}$ as [10]

$$A_{\rm F}(\boldsymbol{p}, \omega) = -{\rm Im}[G_{\rm F}(p, i\omega_F \to \omega + i\delta)]/\pi, \tag{12}$$

$$I_{\rm F}(\boldsymbol{p}, \omega) \propto p^2 A_{\rm F}(\boldsymbol{p}, \omega) f(\omega), \tag{13}$$

respectively, where δ is an infinitesimally small positive number. In this paper, we only consider the Fermi component.

3 Results

The left panels in Fig. 2 show the intensity of the Fermi spectral weight (SW) in the unitary regime ($(k_{\rm F} a_s)^{-1} = 0.1$) of a Bose–Einstein mixture at $T_{\rm BEC}$. In the mass-balanced case shown in panel (a1), in addition to the peak line along the Fermi atomic dispersion ($\omega = \epsilon^{\rm F}_{\boldsymbol{p}} - \mu_{\rm F}$) (A), two other peak structures are seen : (B) sharp peak along the dispersion $\omega = \xi^{\rm CF}_{\boldsymbol{p}} = p^2/(2M) - \mu_{\rm CF}$ of composite molecules (where

$M = m_{\rm F} + m_{\rm B}$ and $\mu_{\rm CF}$ are the molecular mass and the molecular chemical potential, respectively). (C) broad downward peak in the negative energy region around the *hole* dispersion $\omega = -\tilde{\xi}^{\rm B}_{-\boldsymbol{p}}$, where $\tilde{\xi}^{\rm B}_{\boldsymbol{p}} = \xi^{\rm B}_{\boldsymbol{p}} - \Sigma_{\rm B}(\boldsymbol{0}, 0)$. To explain the reason for the appearance of these additional peaks, we conveniently note that the Bose distribution function $n(\tilde{\xi}^{\rm B}_{\boldsymbol{q}})$ is very sharp around $\boldsymbol{q} = 0$ near $T_{\rm BEC}$. The analytic-continued Fermi Green's function can then be approximated to

$$G_{\rm F}(\boldsymbol{p}, \omega^+) \simeq \left[\omega^+ - \xi^{\rm F}_{\boldsymbol{p}} - \frac{Z N^0_{\rm B}}{\omega^+ - \xi^{\rm CF}_{\boldsymbol{p}}} - \left\langle \frac{Z N^0_{\rm CF}}{\omega^+ + \tilde{\xi}^{\rm B}_{\boldsymbol{p}^{\rm CF}_{\rm F} - \boldsymbol{p}}} \right\rangle \right]^{-1}, \tag{14}$$

where $\omega^+ = \omega + i\delta$, $Z = 2\pi/(m_r^2 a_{\rm BF})$. $N^0_{\rm B} = \sum_{\boldsymbol{q}} n(\tilde{\xi}^{\rm B}_{\boldsymbol{q}})$ and $N^0_{\rm CF} = \sum_{\boldsymbol{q}} f(\xi^{\rm CF}_{\boldsymbol{q}})$ are the number of unpaired bosons and that of the composite Fermi molecules, respectively. In Eq. (14), $\langle \cdots \rangle$ means the average over the relative angle between $\boldsymbol{p}$ and $\boldsymbol{p}^{\rm CF}_{\rm F}$, where $\boldsymbol{p}^{\rm CF}_{\rm F}$ is the Fermi momentum of molecular fermions. This angle-average naturally leads to the broad downward peak (C) in Fig. 2 (a1). Equation (14) clearly indicates that the Fermi atomic excitations (A) ($\omega = \xi^{\rm F}_{\boldsymbol{p}}$) are coupled to the Fermi molecular excitations (B) ($\omega = \xi^{\rm CF}_{\boldsymbol{p}}$), with coupling constant $\sqrt{Z N^0_{\rm B}}$. Equation (14) also describes coupling between the Fermi atomic dispersion ($\omega = \xi^{\rm F}_{\boldsymbol{p}}$) with hole-like excitation ($\omega = -\xi^{\rm B}_{-p}$)with coupling constant $\sqrt{Z N^0_{\rm CF}}$.

This characteristic structure in SW still remains in the mass-imbalanced case, as shown in Fig. 2 a2, a3, although detailed spectral structures are different between the two panels : when $m_{\rm B} < m_{\rm F}$ shown in panel (a2), the molecular branch (B) becomes clearer, compared to the downward broad peak in the negative energy region (C). When $m_{\rm B} > m_{\rm F}$ shown in panel (a3), on the other hand, the opposite tendency is seen. This difference can qualitatively be understood as follows : In Eq. (14), the intensity of each peak structure (B) and (C) is determined by the coupling constant $\sqrt{Z N^0_{\rm B}}$ and $\sqrt{Z N^0_{\rm CF}}$, respectively. Since, a composite Fermi molecule is composed of one Fermi atom and one Bose atom, the number of unpaired Bose atoms $N^0_{\rm B}$ is related to the number of Fermi molecules $N^0_{\rm CF}$ as $N - N^0_{\rm B} = N^0_{\rm CF}$. This implies that, when the pair-formation becomes remarkable, the increase in $N^0_{\rm CF}$ makes the hole branch (C) ($\omega = -\xi^{\rm B}_{-p}$) clearer, and the decrease in $N^0_{\rm B}$ suppresses the molecular branch (B). Because the binding energy of a two-body bound molecule equals $E = 1/(2m_r a_s^2)$ and $T_{\rm BEC} \sim (N^0_{\rm B}/\zeta(3/2))^{2/3}/(2\pi m_{\rm B})$ (where $\zeta(3/2) = 2.612$), the ratio $T_{\rm BEC}/E_{\rm b} \propto m_r (N^0_{\rm B})^{2/3}/m_{\rm B}$ indicates that the increase in $m_{\rm B}$ increases the number $N^0_{\rm CF}$ of Bose–Fermi molecules, as well as the increase in the coupling $\sqrt{Z N^0_{\rm CF}}$. Thus, when $m_{\rm B} > m_{\rm F}$, the branch (C) in Fig. 2a3 becomes remarkable compared to the mass-balanced case shown in panel (a1).

Figure 2b1–b3 shows the photoemission spectra (PES). We find that the three-peak structure appearing in SW, as well as above-mentioned mass-imbalanced effects, can be detected by PES. This indicates the possibility of experimental confirmation of the above-mentioned phenomena seen in panels (a1)-(a3) by using this spectroscopic measurement.

4 Summary

To summarize, we have discussed strong-coupling and mass imbalance effects on the single-particle excitation property of an ultracold Bose–Fermi mixture in the unitary regime at T_{BEC}. We numerically evaluated the single-particle spectral weight (SW), as well as the photoemission spectrum (PES) in a ^{23}Na–^{40}K and a ^{87}Rb–^{40}K mixtures. We found that the characteristic three-peak structure in SW that has recently been discussed in a mass-balanced Bose–Fermi mixture succeeds to the mass-imbalanced case. However, the detailed spectral structures are very different between the case of $m_{\mathrm{B}} < m_{\mathrm{F}}$ (^{23}Na–^{40}K) and $m_{\mathrm{B}} > m_{\mathrm{F}}$ (^{87}Rb–^{40}K). We also showed both these spectral structures, as well as mass imbalance effects, can also be seen in PES. Since PES is experimentally accessible in cold atom physics, our results would be useful for clarifying the strong-coupling phenomena in a Bose–Fermi mixture.

Acknowledgements We would like to thank R. Sato for discussions. This work was supported by KiPAS project in Keio University. DI was supported by Grant-in-aid for Scientific Research from JSPS in Japan (No. JP16K17773). YO was supported by Grant-in-aid for Scientific Research from MEXT and JSPS in Japan (Nos. JP16K05503, JP18K11345, JP18H05406).

References

1. C.A. Stan, M.W. Zwierlein, C.H. Schunck, S.M.F. Raupach, W. Ketterle, Phys. Rev. Lett. **93**, 143001 (2004)
2. S. Inouye, J. Goldwin, M.L. Olsen, C. Ticknor, J.L. Bohn, D.S. Jin, Phys. Rev. Lett. **93**, 183201 (2004)
3. M.-J. Zhu, H. Yang, L. Liu, D.-C. Zhang, Y.-X. Liu, J. Nan, J. Rui, B. Zhao, J.-W. Pan, E. Tiemann, Phys. Rev. A **96**, 062705 (2017)
4. J.J. Zirbel, K.-K. Ni, S. Ospelkaus, J.P. D'Incao, C.E. Wieman, J. Ye, D.S. Jin, Phys. Rev. Lett. **100**, 143201 (2008)
5. C.-H. Wu, J.W. Park, P. Ahmadi, S. Will, M.W. Zwierlein, Phys. Rev. Lett. **109**, 085301 (2012)
6. C. Chin, R. Grimm, P. Julienne, E. Tiesinga, Rev. Mod. Phys. **82**, 1225 (2010)
7. The BCS-BEC Crossover and the Unitary Fermi Gas, edited by W. Zwerger (Springer, Berlin, 2012)
8. M. Randeria, in *Bose-Einstein Condensation*, ed. by A. Griffin, D.W. Snoke, S. Stringari (Cambridge University Press, New York, 1995), p. 355
9. S. Tsuchiya, R. Watanabe, Y. Ohashi, Phys. Rev. A **80**, 033613 (2009)
10. S. Tsuchiya, R. Watanabe, Y. Ohashi, Phys. Rev. A **82**, 033629 (2010)
11. D. Kharga, D. Inotani, R. Hanai, Y. Ohashi, J. Phys. Soc. Jpn. **86**, 084301 (2017)
12. J.T. Stewart, J.P. Gaebler, D.S. Jin, Nature (London) **454**, 744 (2008)
13. Y. Sagi, T.E. Drake, R. Paudel, R. Chapurin, D.S. Jin, Phys. Lev. Lett. **114**, 075301 (2015)
14. P. Törmä, Phys. Scr. **91**, 043006 (2016)
15. D. Kharga, H. Tajima, P. van Wyk, D. Inotani, Y. Ohashi, J. Phys. Soc. Jpn. **86**, 074301 (2017)
16. E. Fratini, P. Pieri, Phys. Rev. A **81**, 051605(R) (2010)
17. E. Fratini, P. Pieri, Phys. Rev. A **85**, 063618 (2012)
18. E. Fratini, P. Pieri, Phys. Rev. A **88**, 013627 (2013)
19. A. Guidini, G. Bertanina, E. Fratini, P. Pieri, Phys. Rev. A **89**, 023634 (2014)
20. N.M. Hugenholtz, D. Pines, Phys. Rev. **116**, 489 (1959)